SAND2022-13851C

Actual Field Response Simulation Using Modified Laboratory Loading Conditions

Troy Skousen, Brandon Zwink
Sandia National Laboratories[1]
PO Box 5800 MS-0840
Albuquerque, NM 87185-0840

Jesus Reyes-Blanco, Peter Avitabile
Structural Dynamics and Acoustic Systems Laboratory
University of Massachusetts Lowell
One University Avenue
Lowell, Massachusetts 01854

ABSTRACT

Laboratory qualification tests must replicate field responses, which can be difficult to achieve. A history of vibration qualification test approaches is discussed showing how methods have improved over time starting with single axis methods that were not intended to replicate responses up to recent work where the dynamics of the field and laboratory are characterized and used to generate Multiple Input, Multiple Output test loads for replicating field motion. The goal is to morph the real field loads into equivalent laboratory loads to achieve proper response. The ultimate goal is to simulate realistic damage mechanisms. Recently, impedance and modal modeling techniques have strived to accomplish this, but there are pros and cons to both approaches. This work shows an implementation of the impedance and modal techniques on a simple analytical model. This is the first step to developing a blended technique for conducting appropriate tests in the laboratory to simulate realistic responses.

Keywords: Replicating Responses, Fixture Neutralization (FINE), Impedance Based FINE, Modal Based FINE

INTRODUCTION

The first theme of this paper is to provide historical background to vibration test specifications. How specification started out and incremental changes that have been made to improve the early single axis test methodologies will be discussed. Finally, the discussion will show how test methods are moving away from single axis and heading toward multiple input tests with emphasis on replicating test article responses. The improvements are necessitated by issues that have come up in testing which have caused unnecessary failures in the test article because of poor test design. Many of these problems stem from test boundary conditions that do not allow the test article to move the same way as when fielded and the inaccuracies associated with the derivation of enveloped test specifications with few break points. Major improvements have come in the way of Multiple Input, Multiple Output (MIMO) vibration testing and the dynamic characterization of the test article and test set up. With this historical background in place, a couple of the newer methods, categorized as Fixture Neutralization (FINE), that determine appropriate loads for a test boundary condition to generate replicated test article responses are discussed. The methods shown are from Reyes-Blanco [1] that uses unattached fixture responses with test article and boundary condition drive point impedance Frequency Response Functions (FRFs) and Zwink [2] that uses modal analysis based input/output FRFs of the entire test system. A simple analytical model is used to demonstrate the methods.

Historical Background

In the early days of broadband vibration testing, each test facility implemented their own way of executing tests and accompanying test specifications, for example the United States Army Air Forces Specification No. 41065 [3]. In the beginning,

[1] Sandia National Laboratories is a multimission laboratory managed and operated by National Technology & Engineering Solutions of Sandia, LLC, a wholly owned subsidiary of Honeywell International Inc., for the U.S. Department of Energy's National Nuclear Security Administration under contract DE-NA0003525.

recommendations consisted of sine sweep and sine dwell vibration tests. Sine testing gave way to smooth acceleration-based random vibration spectra for single axis testing. In 1956, Morrow [4] discussed how the smooth test specifications *(i.e., enveloped specifications with few break points)* required by test machines did not make sense given the dynamic nature seen in field test measurements. Morrow explained that the smooth specifications can produce severe responses in the Device Under Test (DUT) while at the same time be inadequate compared to field test measurements depending on the frequency. Also in 1956, Blake [5] discussed another source of severe DUT responses pointing out the need to control or account for the dynamics of the test machines. Blake surmised that the DUT responses were ignored because the dynamics were too difficult to address and recommended that the discrepancies should be accounted for when technology was able to support doing so.

After World War II, the environmental testing community was clamoring for standard qualification testing to replace the various test procedures from each organization [6]. The needs of the United States government were at the forefront of these conversations, so the Department of Defense (DOD) took upon themselves the responsibility to develop a standard. After consulting with the technical community, largely at the Shock and Vibration Exchange which started in 1947, the DOD, led by the Air Force, released MIL-STD-810 [7] in 1962. The focus in the standard was to provide simple and repeatable laboratory tests that would reduce cost. A conscious decision was made to take focus away from methods to correlate laboratory testing with service environments, which would have improved test realism. The work associated with this correlation was seen as an advanced method deemed too complex and extant technologies were not ready to support such activities. The resultant standard specifications were a generic set of straight-line, single axis test specifications, tested sequentially in three axes, for different transportation and delivery platforms. The standard recommended rigid test fixture interfaces connecting the DUT to the test machines for test repeatability. Test specifications were to be evaluated at the interface between the DUT and the fixture. There was no direct connection to the laboratory test dynamic response of the DUT to the field responses, but the specifications were intended to conservatively envelope field environment measurements. These simple specifications were put in place as a starting point with the expectation that during the development of the design, higher fidelity information would be collected and utilized to improve each test environment, raising or lowering frequency content as appropriate. The author's impression is that these adjustments were rare because the necessary information was infrequently collected due to field test instrumentation limitations. Other standards were introduced by other organizations such as the National Aeronautics and Space Administration (NASA) [8] [9], the Aerospace Corporation [10], and the Air Force Space Command [11] to suit needs that were not covered by DOD documents such as addressing environment loads from space craft launch vehicle, for example.

Since the introduction of the vibration test standards, institutions have become aware of the technical issues associated with the simple approach to testing. One scenario often discussed in the vibration test community are designs that have demonstrated proper functionality during usage but fail during laboratory tests. Even during design development before fielded data are available, when test failures happen, investigations often point to test setup or implementation producing very high DUT responses that do not seem appropriate for what is expected in the field. In these situations, proper test design would have avoided the high costs of investigating test failures and the unnecessary changes to designs that may have been suitable for their intended purpose. There is also a possibility that design flaws can escape notice when tests do not faithfully replicate the field DUT responses. Agencies are hesitant to share stories about their test failures and the associated lessons learned. Instead, papers have been published to discuss the improvements made in vibration testing while sometimes mentioning previous failures in passing.

Of these publications on improved testing, there are several methods that work to improve single axis vibration testing. One of the most well-known methods is input force limits at the DUT interface as published by Scharton [12] who said that limiting was necessary due to stiff test machine interfaces and the relatively infinite power imparted by the shakers. In the method, an appropriate maximum interface force holds in check the amount of energy the test machine imparts to the DUT. Acceleration response limiting [13] [14] is related to force limits except that response accelerations on the test structure are limited based on field data, analysis, or intuition. Another method used in single axis testing is to develop a single input, multiple output (SIMO) model of the DUT to find an input that best matches the combined responses desired on the test article [15] [16]. The limiting methods address the symptomatic problems associated with straight line test specifications and impedance mismatch between the laboratory and field configurations that cause high DUT responses. The current version of MIL-STD-810H [17] includes recommended practices for force control and acceleration response limiting. Utilizing the SIMO method helps prevent high and low DUT responses. These methods put a "band-aid" fix on and do not address the underlying problem that the inputs are not correct for the DUT in the laboratory.

Even though single axis testing with large vibration shakers still seems to be the norm for design development and qualification, research and technology improvements are making multiple input, multiple output (MIMO) testing more viable. The test specifications for MIMO tests are much more involved than single axis testing as the specifications must address the phase and coherence relationships between the control channels. MIMO testing started with using two shakers to excite the DUT in the same direction as discussed by Cap [18] and Gregory [19]. Three and six degree-of-freedom base excitation testing is gaining popularity [20] [21]. These tests are more accurate if the DUT is attached at one interface location and has the additional benefit

of only needing one test setup instead of three single axis setups. Daborn [22] [23] [24] [25] introduced Impedance Matched, Multi-Axis Testing (IMMAT). Others such as Mayes [26] and Schultz [27] have continued researching the IMMAT technique. In the IMMAT method, a DUT is attached to a fixture that is dynamically like the field boundary condition and positionable shakers are placed around the test setup to excite the DUT either directly or through the fixture. The several variants of MIMO testing have shown vast improvements in the response characteristics compared to single axis testing. The current version of MIL-STD-810H [17] includes recommended practices for multiple input test methods. With MIMO, desired responses can be achieved more accurately at many locations across the DUT. Yet, these techniques focus on matching more responses at specific locations instead of characterizing and matching the dynamic response of the system.

Several writers such as McConnell [28] and Avitabile [29] have pointed out that characterizing the dynamic differences between the laboratory and the field is necessary for making requisite adjustments to the test design to improve specifications, control scheme, and/or fixture design. A couple of Fixture Neutralization methods presented by Reyes-Blanco [1] [30] [31] and Zwink [2] [32] are included in MIMO testing category. The Impedance Based FINE method from Reyes-Blanco relies on frequency response function (FRF) substructuring and requires characterizing the DUT and the fixtures separately. By comparison, the Modal Based FINE method from Zwink utilizes the whole system dynamics to achieve equivalent results when the test has the appropriate rank of excitation and response degrees of freedom. Both methods have advantages and disadvantages especially when used with imperfect test data. In a future work, the author plans to blend the methods together to take advantage of benefits found in each method. The ability to reproduce desired DUT responses will alleviate test inaccuracies that cause false test failures and false test passes.

With the historical background set for test method and specification developments, the next section references some theoretical background for the more advanced test methods. Several models are developed to show the use of the Impedance and Modal Based FINE approaches to illustrate the need for adjustments to the test specification to accurately portray the field environment in the laboratory setting.

THEORETICAL BACKGROUND

This section contains some basic definitions and theoretical equations related to the Impedance and Modal Based FINE approaches used for the models presented in this paper.

FRF

The FRF is the ratio of the output response of a structure due to an applied force [33].

$$[H] = \frac{\{x\}}{\{F\}} \tag{1}$$

In Equation (1), [H] is the FRF, {x} is the physical response vectors, and {F} is the physical force applied to the structure. Note that (1) can be rewritten in an equivalent form as

$$[H] = \frac{\{x\}}{\{F\}} = \frac{1}{[M]\left(-\omega^2 + 2j\omega_n\varsigma\omega + {\omega_n}^2\right)} \tag{2}$$

In Equation (2), [M] is the system mass, {ω} is the frequency vector of the FRF, {ω_n} is the system natural frequencies, and ς is the percent of critical damping. As indicated by Zwink [2], with a modal transformation Equation (2) can be looked at in modal space and treated as a sum of independent single degree-of-freedom modal systems. This equation is shown for the k^{th} mode as

$$\left[\bar{H}_k\right] = \frac{\{\bar{x}_k\}}{\{\bar{F}_k\}} = \frac{1}{\left[\bar{M}_k\right]\left(-\omega^2 + 2j\omega_{n_k}\varsigma_k\omega + {\omega_{n_k}}^2\right)} \tag{3}$$

For Equation (3), the bar over the variables signifies values in modal space. Equation (3) can be brought to physical space with

$$[H] = \frac{\{x\}}{\{F\}} = [U]\begin{bmatrix} \bar{H}_1 & & \\ & \bar{H}_2 & \\ & & O \end{bmatrix}[U]^T \tag{4}$$

In Equation (4), [U] is the mode shape matrix for the system.

Dynamic Substructuring

Dynamic substructuring utilizes pieces of models, potentially of varying sources to create or adjust assembled models. De Klerk [34] summarized the various substructuring techniques in a common nomenclature. Substructures are included in several methods that have been provided to generate better inputs for random vibration tests as shown by Mayes [35] , Skousen [36] [37], and Reyes-Blanco [1].

Fixture Neutralization (FINE) Methods

Fixture neutralization methods seek to replicate responses in a DUT due to a load in one boundary condition by determining a new set of loads for another boundary condition. Two variants of the method will be discussed, namely the Impedance Based FINE and the Modal Based FINE.

Impedance Based FINE

Reyes-Blanco [1] developed the Impedance Based Fixture Neutralization method to derive input forces for a DUT with defined boundary conditions that produce the same response measured with another boundary condition under a load. In the method, the response of the first boundary condition under the load is determined without the DUT at the connection degrees-of-freedom. Then the motion of the unattached second boundary condition that will produce the same DUT response is determined using connection degree-of-freedom drive point impedances of the DUT and each boundary condition. The equation is given as

$$\left\{x_c^{(L_2)}\right\} = \left(H_{cc}^{(D)} + H_{cc}^{(L_2)}\right)\left(H_{cc}^{(D)} + H_{cc}^{(L_1)}\right)^g \left\{x_c^{(L_1)}\right\} \tag{5}$$

In Equation (5), superscripts D, L_1, and L_2 represent the DUT, the fixture that provides the first boundary condition (the field configuration), and the fixture that provides the second boundary condition (the laboratory test configuration), respectively. The connection degrees-of-freedom between the DUT and the fixtures are represented by subscript c. The nomenclature for the generalized inverse is given by superscript g. So $\left[H_{cc}^{(D)}\right]$ is the drive point impedance FRF for the DUT at the connection degrees-of-freedom and $\left\{x_c^{(L_2)}\right\}$ is the connection degrees-of-freedom responses of the unconnected L_2 fixture from the load at the input location that is required to make the DUT respond the same way when attached to the L_1 fixture under the original load. The input loads for the L_2 fixture that will produce the desired DUT response are determined with

$$\left\{F_j^{(L_2)}\right\} = \left[H_{cj}^{(L_2)}\right]^g \left\{x_c^{(L_2)}\right\} \tag{6}$$

In Equation (6), subscript j is the input degrees-of-freedom on the fixture and {F} is the applied force so that $\left\{F_j^{(L_2)}\right\}$ is the force applied to the L_2 fixture to achieve the desired response on the DUT. Note that $\left[H_{cj}^{(L_2)}\right]$ is the unattached fixture impedance FRF from the input locations to the connection locations.

Modal Based FINE

The Modal Based Fixture Neutralization method, developed by Zwink [2], provides a way for DUT connection degree-of-freedom forces to match connection forces from a field environment with a different (laboratory) boundary condition without measuring the connection responses nor forces. If the connection forces are the same, then the DUT response will be the same. The Modal method is based on understanding the modal relationship of both the field and laboratory test full system modes and using the resultant FRFs to account for the differences between them. The Modal FINE method is given as

$$\left\{F_j^{(DL_2)}\right\} = \left[H_{ij}^{(DL_2)}\right]^g \left\{x_i^{(DL_1)}\right\} \tag{7}$$

In Equation (7), superscript DL together represent the joined system of the DUT and one of the fixtures and subscript i represents the response location on the DUT. In this case, $\left[H_{ij}^{(DL_2)}\right]$ is physical space FRF derived through the modal space

FRF by Equation (4) of the laboratory test configuration. The advantage of formulating the FRF through modal space is that the Modal Amplitude Contribution Map (MACM) can be developed that describes which laboratory test modes are utilized to replicate the field environment response on a mode-by-mode basis. The MACM is discussed and demonstrated by Zwink [2].

For both FINE methods described above, the number of connection degrees-of-freedom is important. To find a solution, there must be at least as many DUT response degrees-of-freedom as there are active connection degrees-of-freedom. There must also be at least as many input degrees-of-freedom as active connection degrees-of-freedom.

The next section will present a set of analytical models to illustrate the application of the techniques, the need to adjust the input going from field to lab to have the proper DUT desired response and how the response is incorrectly achieved if no adjustments are made.

MODEL DESCRIPTION

To demonstrate the FRF Impedance and Modal Fixture Neutralization methods, a spring and mass model was created in MATLAB [38]. The system configuration A (field configuration) is shown in Figure 1. The model consists of two components: 1) the Base component with 3 springs and 3 masses and 2) the DUT with 3 springs and 4 masses. System configuration A involves connecting the components at two locations where the Base m_1 is connected to the DUT m_4 and the Base m_3 is connected to DUT m_5. The Base serves as a field configuration fixture for the DUT. Table 1 lists the values of the masses and the stiffnesses in the models, which are the same for all springs and the same for all masses.

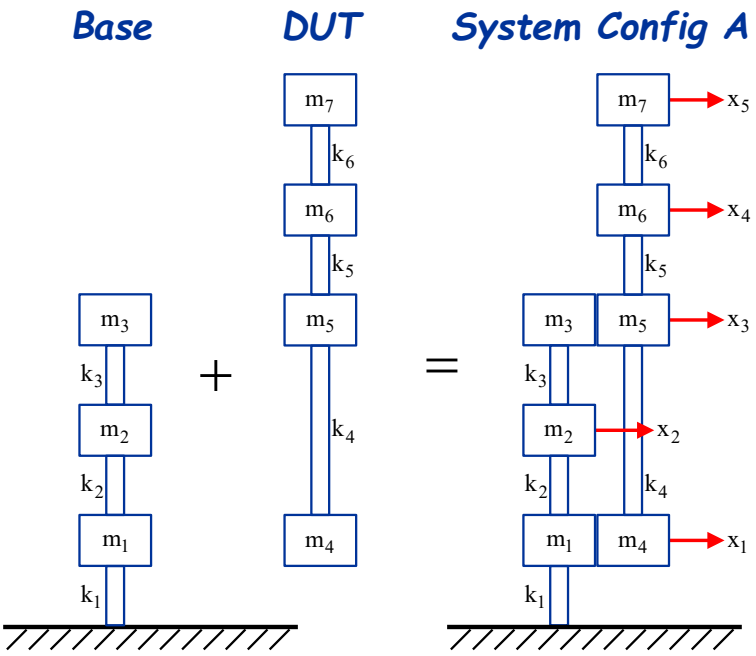

Figure 1. Test model in system the field configuration A

Table 1. Model Properties

Property	Value	Units
Mass (m_i)	0.037	blobs
Stiffness (k_i)	2540	lb./in

The mass and stiffness of the analytical models are given as

$$\begin{bmatrix} m_1 & 0 & 0 \\ 0 & m_2 & 0 \\ 0 & 0 & m_3 \end{bmatrix} \begin{Bmatrix} \ddot{x}_1 \\ \ddot{x}_2 \\ \ddot{x}_3 \end{Bmatrix} + \begin{bmatrix} k_1 + k_2 & -k_2 & 0 \\ -k_2 & k_2 + k_3 & -k_3 \\ 0 & -k_3 & k_3 \end{bmatrix} \begin{Bmatrix} x_1 \\ x_2 \\ x_3 \end{Bmatrix} = \begin{Bmatrix} 0 \\ 0 \\ 0 \end{Bmatrix} \tag{8}$$

$$\begin{bmatrix} m_4 & 0 & 0 & 0 \\ 0 & m_5 & 0 & 0 \\ 0 & 0 & m_6 & 0 \\ 0 & 0 & 0 & m_7 \end{bmatrix} \begin{Bmatrix} \ddot{x}_4 \\ \ddot{x}_5 \\ \ddot{x}_6 \\ \ddot{x}_7 \end{Bmatrix} + \begin{bmatrix} k_{Soft}+k_4 & -k_4 & 0 & 0 \\ -k_4 & k_4+k_5 & -k_5 & 0 \\ 0 & -k_5 & k_5+k_6 & -k_6 \\ 0 & 0 & -k_6 & k_7 \end{bmatrix} \begin{Bmatrix} x_4 \\ x_5 \\ x_6 \\ x_7 \end{Bmatrix} = \begin{Bmatrix} 0 \\ 0 \\ 0 \\ 0 \end{Bmatrix} \quad (9)$$

Equation (8) and Equation (9) are the Base and DUT equations of motion, respectively. In the equations, x_i are the motion degrees-of-freedom and m_i and k_i are the masses and stiffnesses respectively. In the DUT equation, k_{Soft} is a soft spring added to the bottom of the model to keep the DUT loosely anchored to ground (essentially as a free-free component). Table 2 shows the modal properties of each component model.

Table 2. Modal properties of the components

Component	Natural Frequencies	Mode Shapes
Base	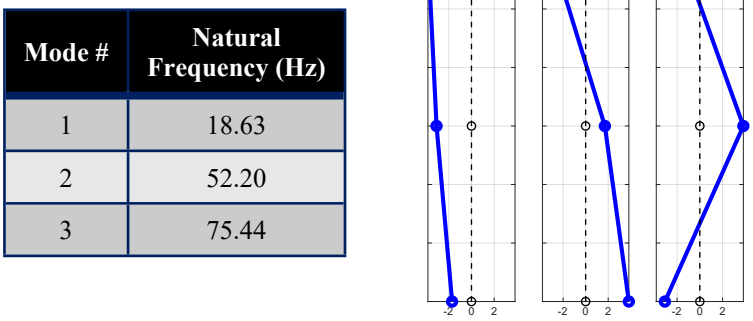	
DUT	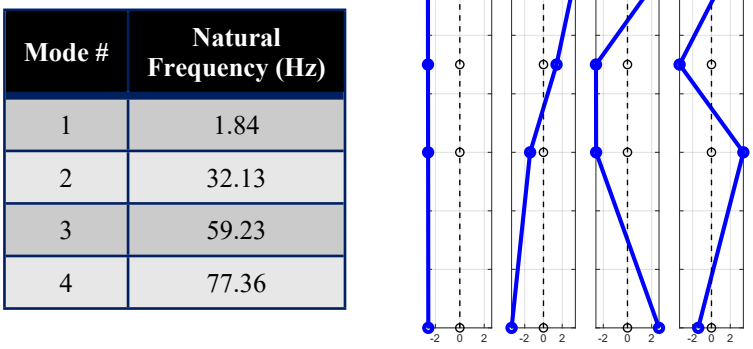	

The system configuration A (field) is given as

$$\begin{bmatrix} m_1+m_4 & 0 & 0 & 0 & 0 \\ 0 & m_2 & 0 & 0 & 0 \\ 0 & 0 & m_3+m_5 & 0 & 0 \\ 0 & 0 & 0 & m_6 & 0 \\ 0 & 0 & 0 & 0 & m_7 \end{bmatrix} \begin{Bmatrix} \ddot{x}_1 \\ \ddot{x}_2 \\ \ddot{x}_3 \\ \ddot{x}_4 \\ \ddot{x}_5 \end{Bmatrix} +$$
$$\begin{bmatrix} k_1+k_2+k_4 & -k_2 & -k_4 & 0 & 0 \\ -k_2 & k_2+k_3 & -k_3 & 0 & 0 \\ -k_4 & -k_3 & k_3+k_4+k_5 & -k_5 & 0 \\ 0 & 0 & -k_5 & k_5+k_6 & -k_6 \\ 0 & 0 & 0 & -k_6 & k_6 \end{bmatrix} \begin{Bmatrix} x_1 \\ x_2 \\ x_3 \\ x_4 \\ x_5 \end{Bmatrix} = \begin{Bmatrix} 0 \\ 0 \\ 0 \\ 0 \\ 0 \end{Bmatrix} \quad (10)$$

As part of the assembly process for Equation (10), the soft spring, k_{Soft}, is removed from the DUT model. Figure 2 shows the model in configuration B. The only difference from configuration A is that instead of m_4 from the DUT connecting to m_1 in the Base, m_4 now connects to m_2 on the Base. The spring stiffnesses do not change. Graphically the length of k_4 has changed, but spring length is not part of the model and is used for illustrative purposes only.

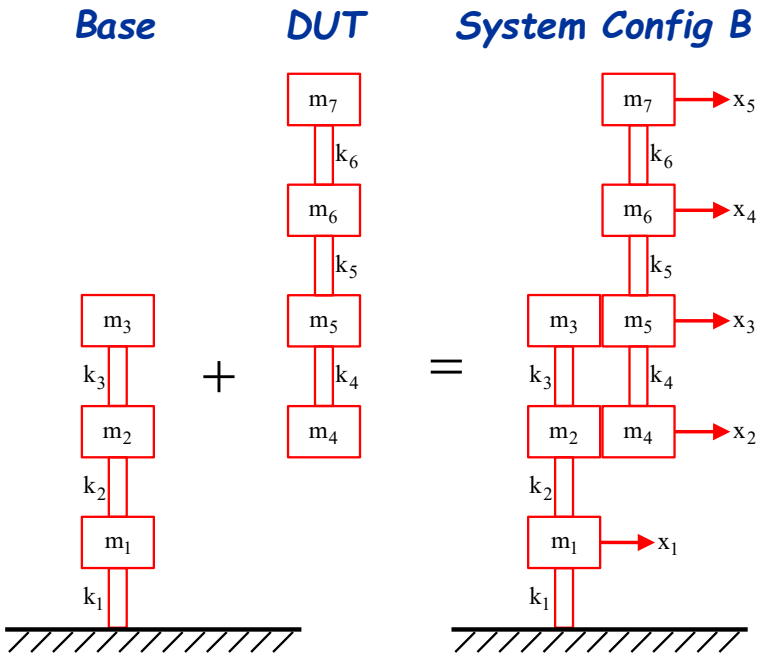

Figure 2. Test model in system laboratory test configuration B

The system configuration B (laboratory) is given as

$$\begin{bmatrix} m_1 & 0 & 0 & 0 & 0 \\ 0 & m_2+m_4 & 0 & 0 & 0 \\ 0 & 0 & m_3+m_5 & 0 & 0 \\ 0 & 0 & 0 & m_6 & 0 \\ 0 & 0 & 0 & 0 & m_7 \end{bmatrix} \begin{Bmatrix} \ddot{x}_1 \\ \ddot{x}_2 \\ \ddot{x}_3 \\ \ddot{x}_4 \\ \ddot{x}_5 \end{Bmatrix} +$$
$$\begin{bmatrix} k_1+k_2 & -k_2 & 0 & 0 & 0 \\ -k_2 & k_2+k_3+k_4 & -k_3-k_4 & 0 & 0 \\ 0 & -k_3-k_4 & k_3+k_4+k_5 & -k_5 & 0 \\ 0 & 0 & -k_5 & k_5+k_6 & -k_6 \\ 0 & 0 & 0 & -k_6 & k_6 \end{bmatrix} \begin{Bmatrix} x_1 \\ x_2 \\ x_3 \\ x_4 \\ x_5 \end{Bmatrix} = \begin{Bmatrix} 0 \\ 0 \\ 0 \\ 0 \\ 0 \end{Bmatrix} \quad (11)$$

Note the differences between the equations for system A and B (Equation (10) to Equation (11)) which are due to the change in the connection location. Table 3 compares the natural frequencies between system configuration A and B. Figure 3 compares the mode shapes between system configuration A and B. Note that the elongated springs are for display purposes only and have no effect on the models. For both the table and the figure, blue shows system A and red shows system B. The circle marker represents the Base masses. The X marker represents the DUT masses. A circle and an X marker together represent connected masses. Therefore, a red circle with an X indicates connected masses from the Base and the DUT for system configuration B.

Table 3. System A vs System B natural frequencies

Mode Number	System A (Field) Natural Frequency (Hz)	System B (Laboratory) Natural Frequency (Hz)
1	13.1	10.9
2	31.3	30.9
3	56.6	54.8
4	66.5	66.9
5	72.5	74.0

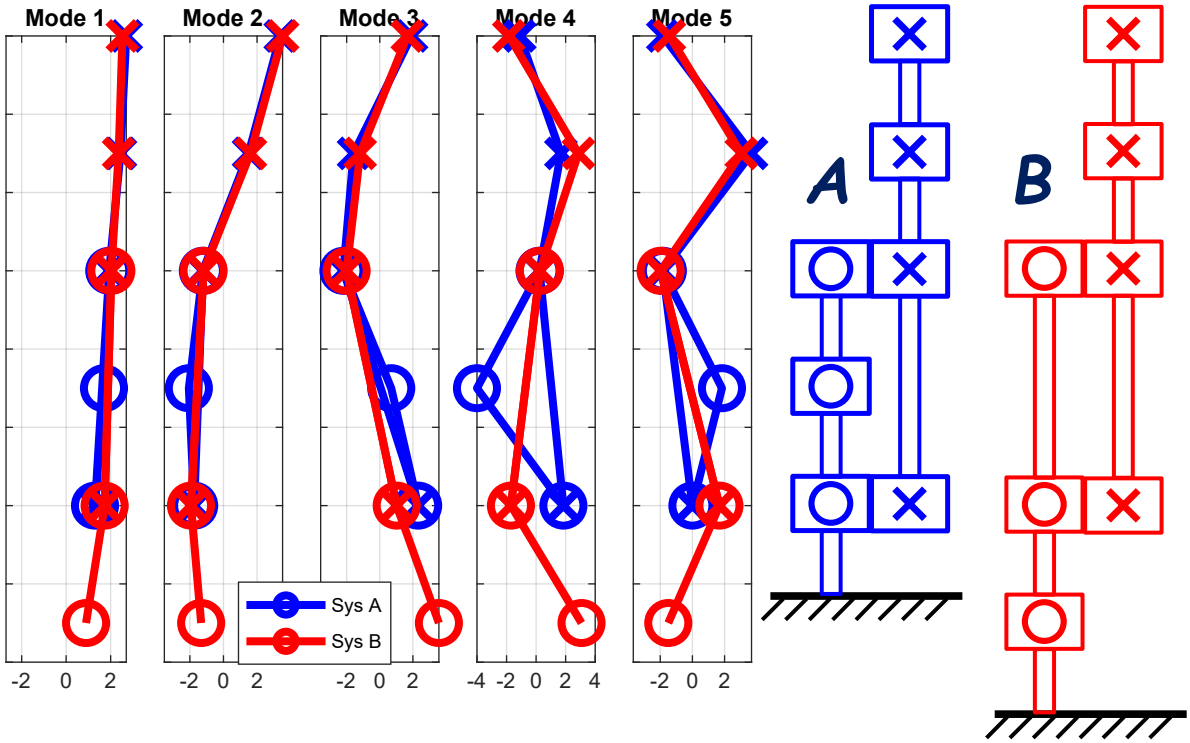

Figure 3. Field System A (blue) vs Laboratory System B (red) mode shapes. O's are the Base masses and X's are the DUT masses. When an X and an O are together, the masses from the Base and the DUT are connected. The system configurations A and B are represented graphically to the right of the mode shape plots.

The next section provides some case studied for the FINE methods previously discussed using the model just described. First the models are used to show how applying the same loads to both models generate different DUT responses. With the goal to replicate the DUT response a new load must be determined for the system B (laboratory) configuration, provided by the FINE methods in independent test cases.

TEST CASES STUDIED

The following test cases are presented

- Test Case 1: Applying the same load to the Field System A and the Laboratory System B
- Test Case 2: Impedance Based FINE
    - Test Case 2, Part 1: Determining the unloaded Base motion for Field and Laboratory
    - Test Case 2, Part 2: Poor DUT response with insufficient loads
    - Test Case 2, Part 3: Desired DUT response with sufficient loads
- Test Case 3: Modal Based FINE

Test Case 1: Applying the same load to the Field (System A) and the Laboratory (System B)

As a starting point to the case studies, the same load is applied to the bottom mass or degree-of-freedom of the Base for both systems. Figure 4 shows the haversine force applied to the structures. The full duration pulse time history is shown in the top left and the time history zoomed into the nonzero pulse content is on the top right. The bottom plot is the force spectrum. The diagrams on the right show where the load is applied on m_1 to both model configurations.

Figure 5 and Figure 6 compare the DUT responses of each system under the load. Recall that the only difference between the two systems is the connection degree-of-freedom that DUT m_4 is attached to in the Base: m_1 for system A and m_2 for system B. There is one set of plots for each DUT degree-of-freedom. The legend describes which system model degree-of-freedom each one applies to. Each plot is also aligned to the appropriate DUT degree-of-freedom in the schematic on the right. Despite such a seemingly minor change, the DUT responses are not the same.

The following test cases show how the FINE methods will replicate the DUT response for both configurations, which is not possible if no adjustments are made. New loads must be determined. The next test case shows an implementation of the Impedance method.

Test Case 2: Impedance Based FINE

Recall that for the Impedance Based FINE, the connection drive point FRFs of the DUT and the next assembly (the Base) are used to derive new loads for the System B, laboratory configuration to replicate the DUT response in the laboratory configuration.

Test Case 2, Part 1: Determining the unloaded Base motion for Field and Laboratory

The first step in the Impedance Based FINE method is to determine the response of the connection degrees-of-freedom of the unattached Base component for system A. This is done by applying the load from Figure 4 to m_1 on the Base component model without the DUT to obtain the connection degree-of-freedom responses. Then Equation (5) is used to determine the unattached connection degree-of-freedom response for the Base in the laboratory test, system B configuration needed to reproduce the DUT motion. Figure 7 and Figure 8 compare the time histories and the spectra for the acceleration motion for the unattached Base connection degrees-of-freedom. For system A, the unattached Base connection degree-of-freedom motion due to the original input is shown. For system B, the derived motion of the unattached connection degrees-of-freedom is shown. Now the process to generate the loads required to generate the unloaded connection responses for System B is demonstrated.

Test Case 2, Part 2: Poor DUT response with insufficient loads

With the unattached Base connection degrees-of-freedom motion for System B in hand, Equation (6) is used to determine the new loads to drive the same DUT response from System A in System B. At this point, a choice needs to be made about which Base input degrees-of-freedom will be used to load system B. If only one load is applied at m_2 on the Base, the new input force is determined and shown in Figure 9. Figure 10 shows the system B DUT responses to the load, which do not match the system A DUT responses. Not enough unique input loads were applied as at least the same number of unique loading degrees-of-freedom are required for each connection degree-of-freedom. There are two connection degrees of freedom, so at least two input degrees of freedom are required, which will be shown next.

Test Case 2, Part 3: Desired DUT response with sufficient loads

To correct the problem of not enough distinct loads applied to the Base, loads are now applied to Base m_2 and m_3 in the System B configuration. Figure 11 and Figure 12 show the spectral and time history forces determined from Equation (6). Applying the load at two locations satisfies the requirement to have one input degree-of-freedom for each connection degree-of-freedom. Applying these loads to System B, the time history and spectral DUT responses are generated and seen in Figure 13 and Figure

14 respectively with the original DUT responses for reference. With two input loads, the system B DUT responses match the original system A responses.

Having shown a successful implementation of the Impedance Based FINE method, the same will be shown for the Modal Based FINE.

Test Case 3: Modal Based FINE

The same rules regarding the number of input loads apply for the Modal Based FINE method that were demonstrated for the Impedance Based FINE method. The Modal Based FINE method will be shown with the same Base input degrees-of-freedom as were used for the Impedance method.

The first step in the Modal Based method is to determine the DUT responses due to the input load in system A. With those responses, Equation (7) is used to derive the inputs to system B required to match the DUT responses. Figure 15 and Figure 16 show the spectra and time history plots respectively for the new loads on Base m_2 and m_3. Note that the loads look very similar if not identical to the loads determined from the Impedance method. Figure 17 and Figure 18 show the time history and spectra responses of the system B DUT with the input provided by the Modal method. The system B responses match the original system A responses very well.

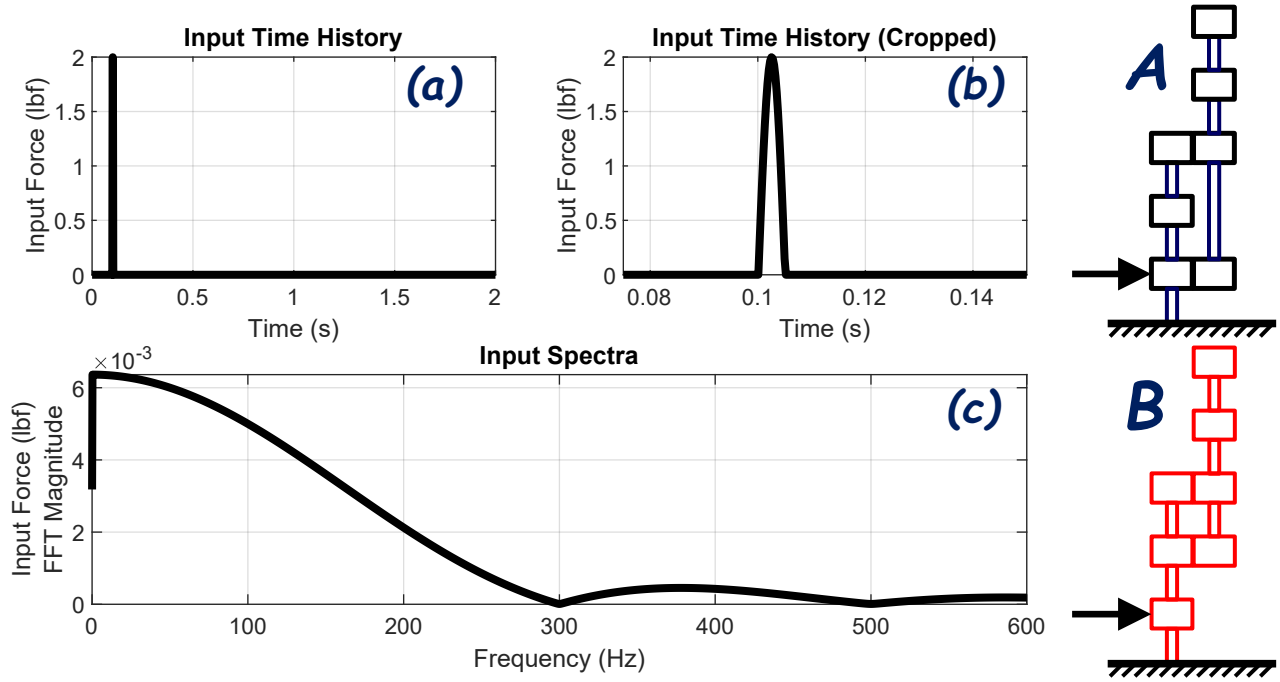

Figure 4. Initial input force. The top two plots (a & b) are time history plots with (b) zoomed in to the pulse. The bottom plot (c) is the spectrum of the pulse. The graphics on the right show where the load is applied to each model configuration.

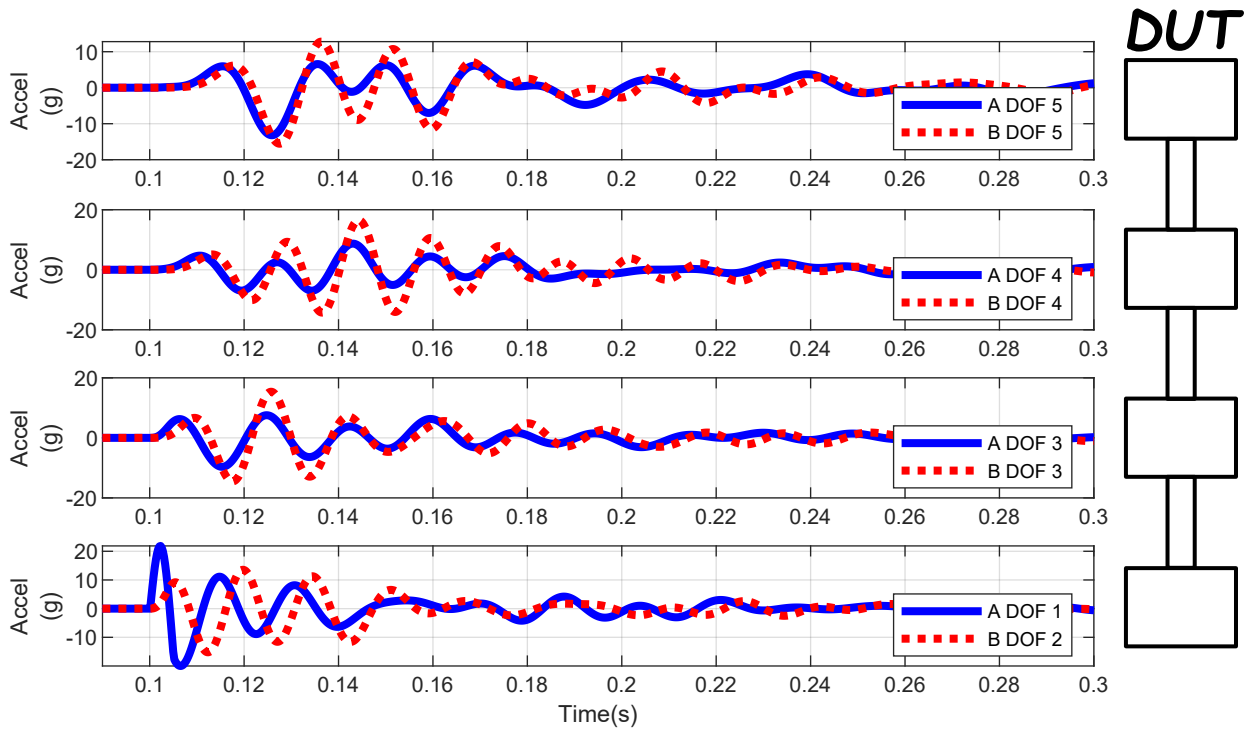

Figure 5. Time domain DUT response in System A and B with the same input. The legend shows which system degree-of-freedom corresponds to each sub plot which in turn corresponds to the degrees-of-freedom in the DUT graphic to the right of the plots. The goal is for the DUT response to be the same for both Systems.

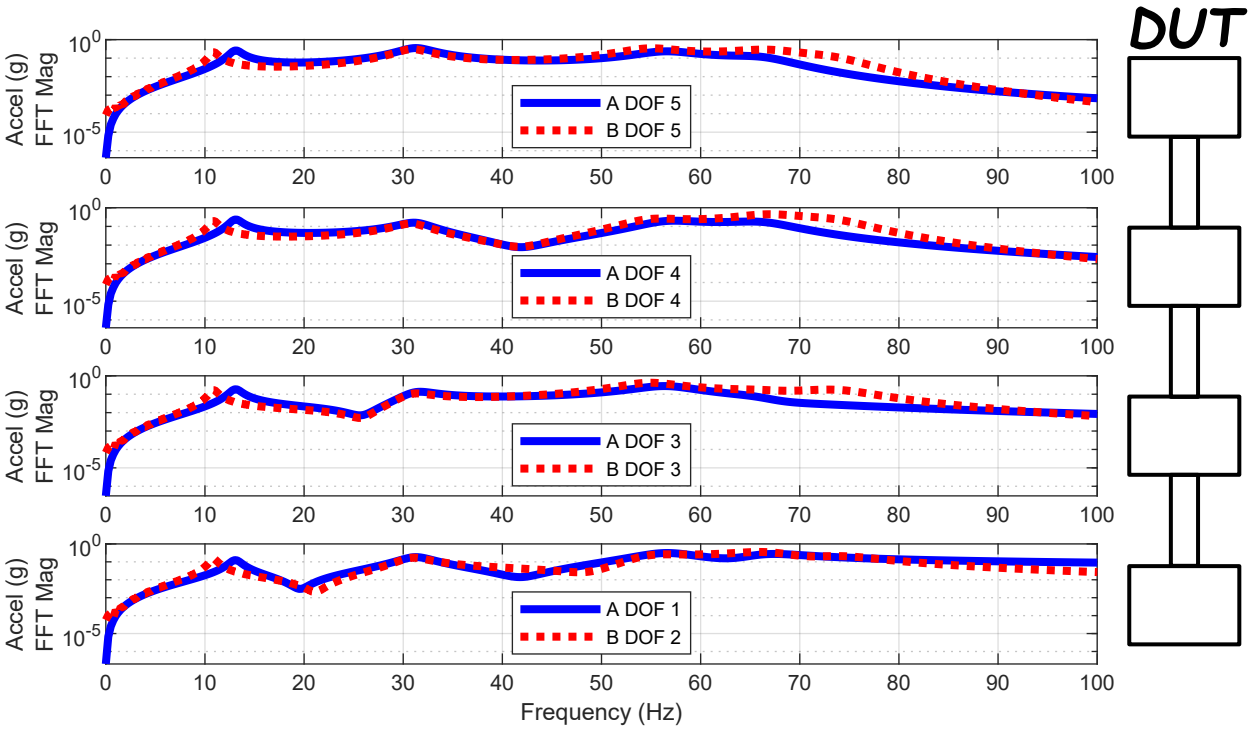

Figure 6. Frequency domain DUT response in System A and B with the same input. The legend shows which system degree-of-freedom corresponds to each sub plot which in turn corresponds to the degrees-of-freedom in the DUT graphic to the right of the plots. The goal is for the DUT response to be the same for both Systems.

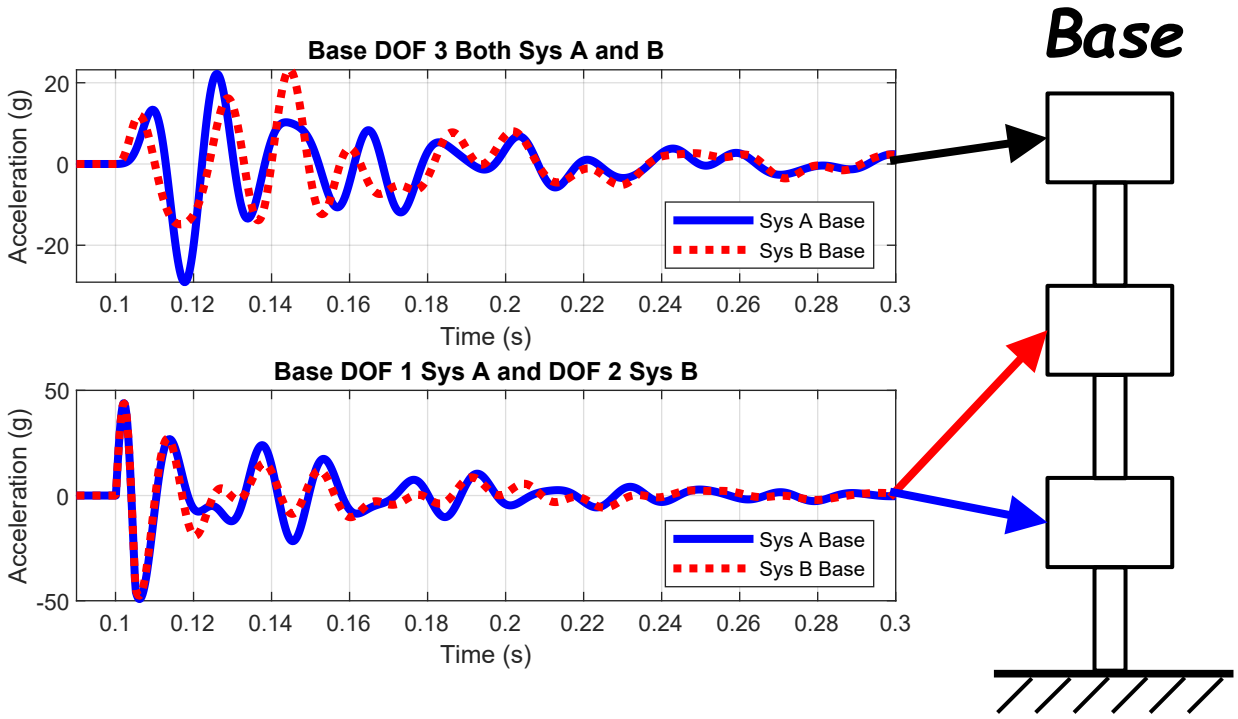

Figure 7. Comparison of unattached boundary connection acceleration time histories required to produce the loads that will generate the same DUT response. System A connection location consists of Base DOF 1 (blue arrow) & 3 (black arrow) and DOF 2 (red arrow) & 3 (black arrow) for System B.

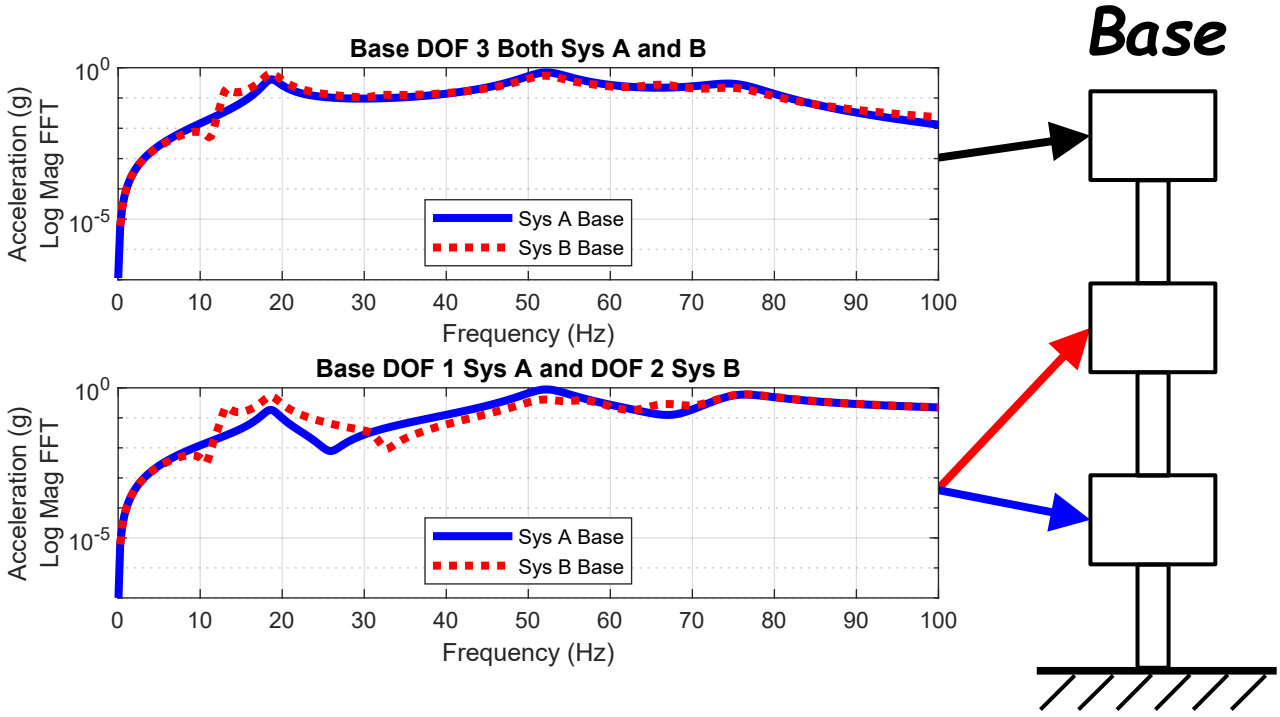

Figure 8. Comparison of unattached boundary connection acceleration spectra required to produce the loads that will generate the same DUT response. System A connection location consists of Base DOF 1 (blue arrow) & 3 (black arrow) and DOF 2 (red arrow) & 3 (black arrow) for System B.

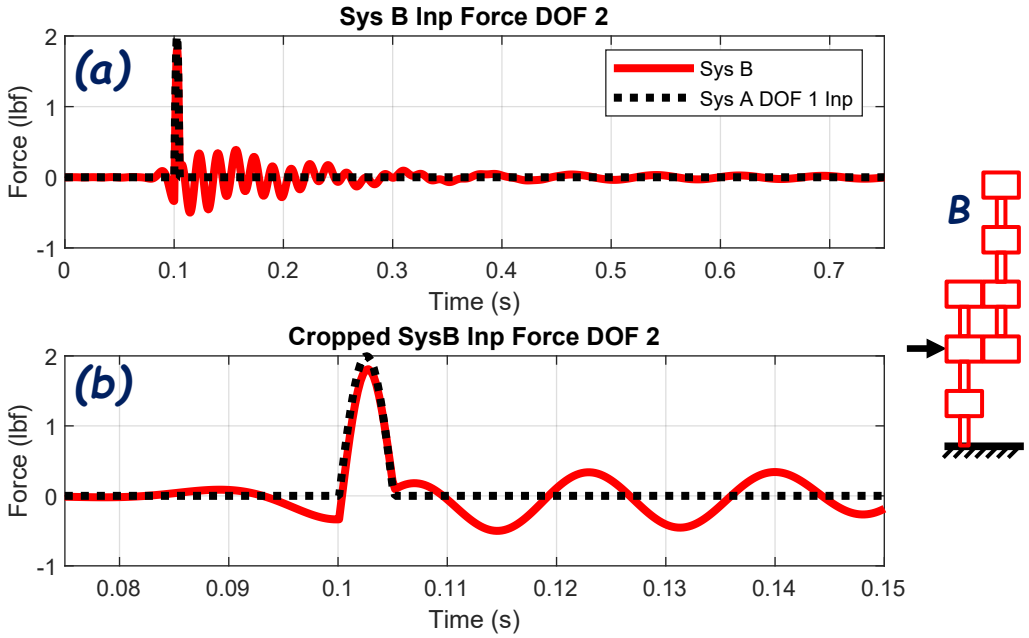

Figure 9. Input force from Equation (6) for the Impedance Based FINE method if only one input us implemented on system B at m_2. The top plot (a) is the time history, and the bottom plot (b) is the time history zoomed into the main pulse of the load. The schematic on the right shows where the input is applied on System B.

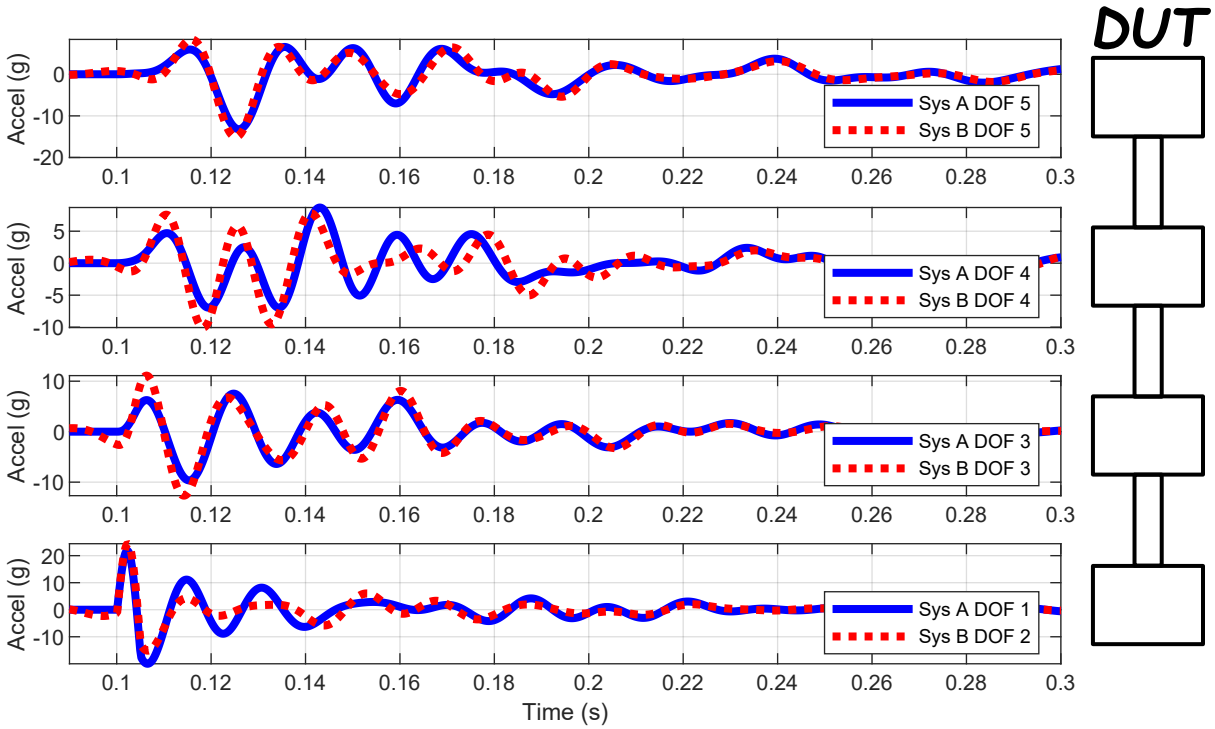

Figure 10. DUT responses in System B using the Impedance FINE method if only one derived input load is applied at degree-of-freedom 2. The legend shows which system degree-of-freedom corresponds to each sub plot which in turn corresponds to the degrees-of-freedom in the DUT graphic to the right of the plots. The goal is for the DUT response to be the same for both Systems.

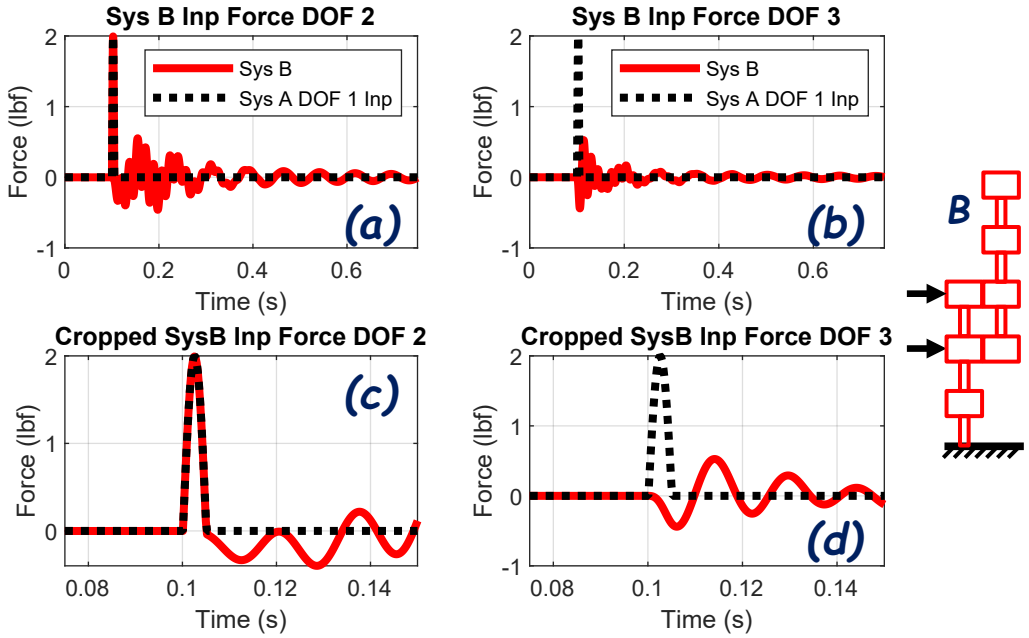

Figure 11. New system B force input time history from the Impedance FINE method to replicate DUT response from system A, plotted with the original system A input for reference. On the left (a & c) is shown the load derived for DOF 2 (m_2) and on the right (b & d) is the load for DOF 3 (m_3). The bottom row (c & d) is the same time histories from above but zoomed into the main pulse.

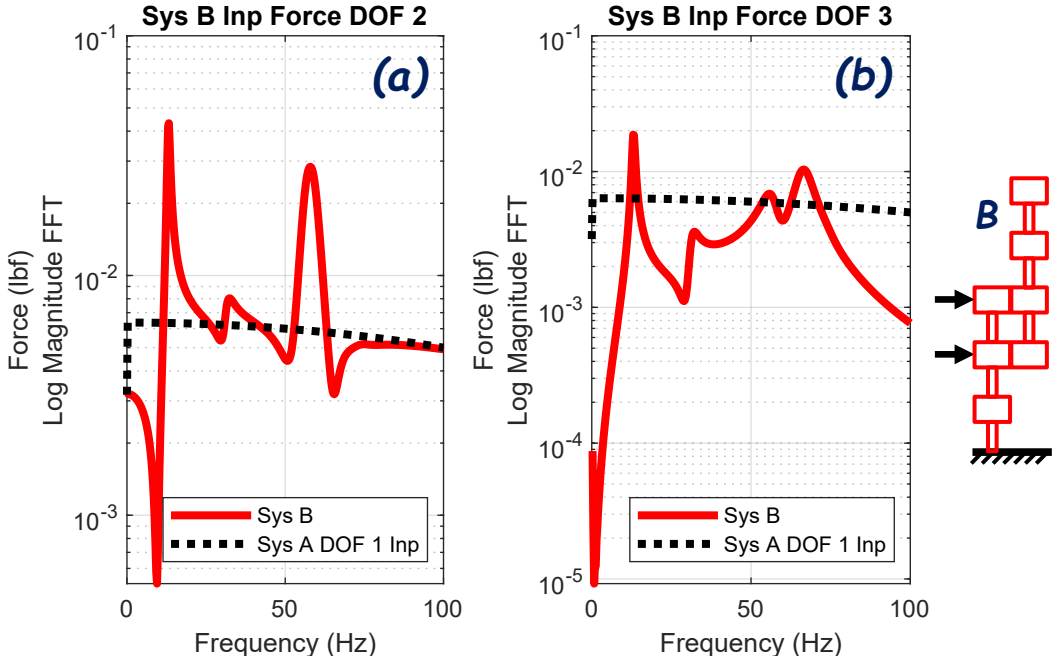

Figure 12. New system B force input spectra from the Impedance FINE method to replicate DUT response from system A, plotted with the original system A input for reference. On the left (a) is shown the load derived for DOF 2 (m_2) and on the right (b) is the load for DOF 3 (m_3).

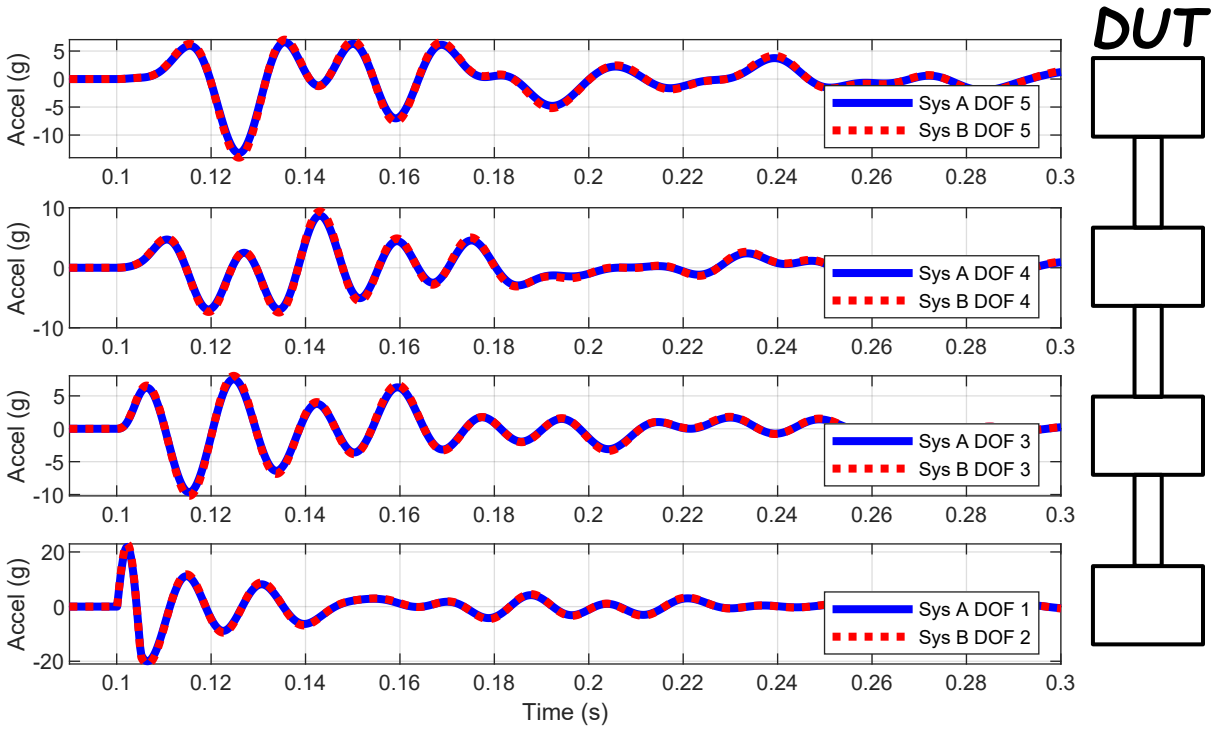

Figure 13. System B, DUT time history response with Impedance FRF derived input compared to original DUT response in system A. The legend shows which system degree-of-freedom corresponds to each sub plot which in turn corresponds to the degrees-of-freedom in the DUT graphic to the right of the plots. The DUT responses are the same for both Systems.

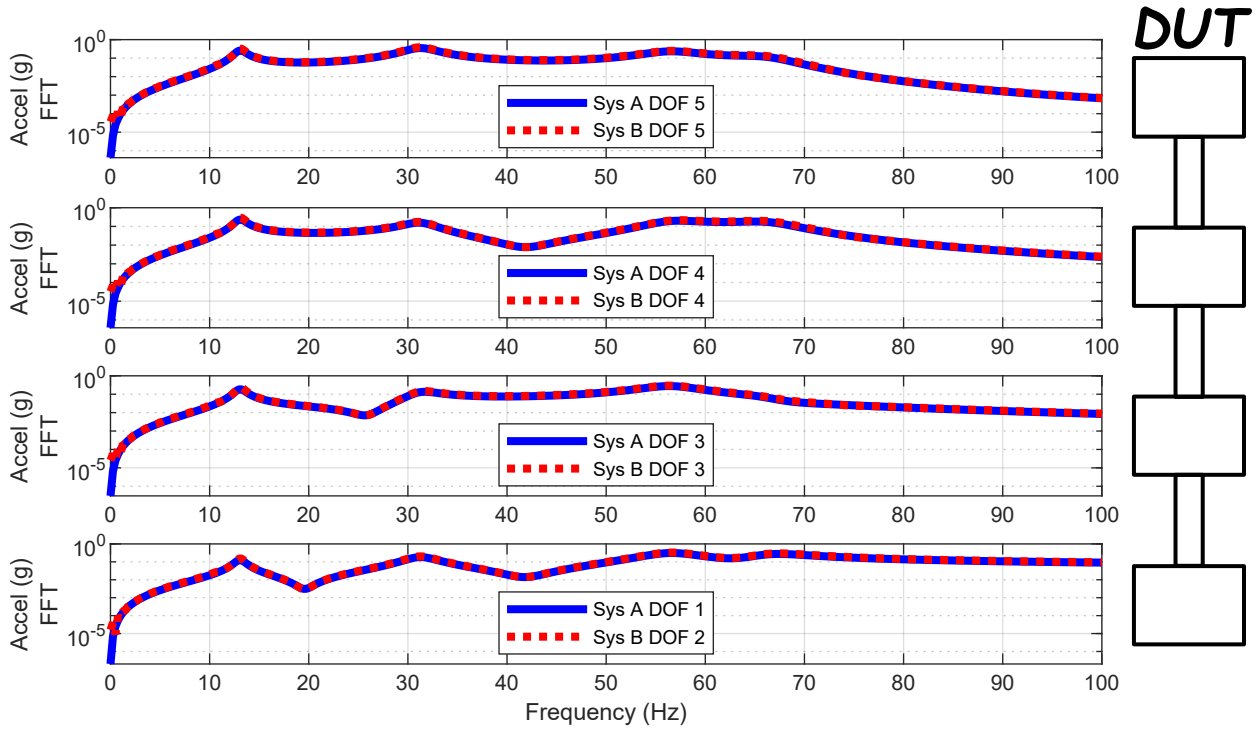

Figure 14. System B, DUT spectral response with Impedance FRF derived input compared to original DUT response in system A. The legend shows which system degree-of-freedom corresponds to each sub plot which in turn corresponds to the degrees-of-freedom in the DUT graphic to the right of the plots. The DUT responses are the same for both Systems.

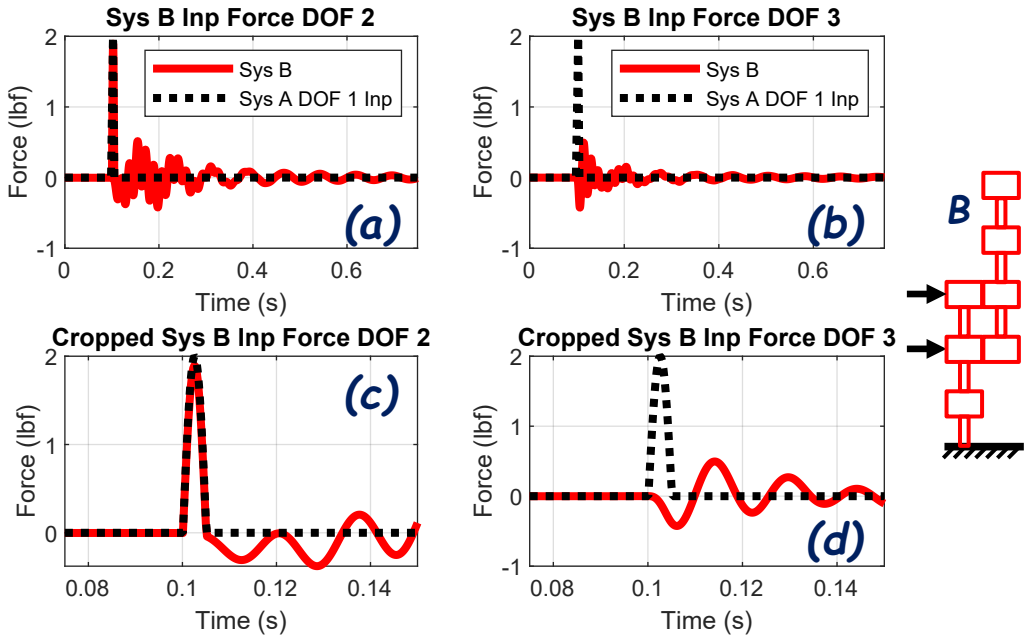

Figure 15. New system B force input time history from the Modal FINE method to replicate DUT response from system A, plotted with the original system A input for reference. On the left (a & c) is shown the load derived for DOF 2 (m_2) and on the right (b & d) is the load for DOF 3 (m_3). The bottom row (c & d) is the same time histories from above zoomed into the main pulse.

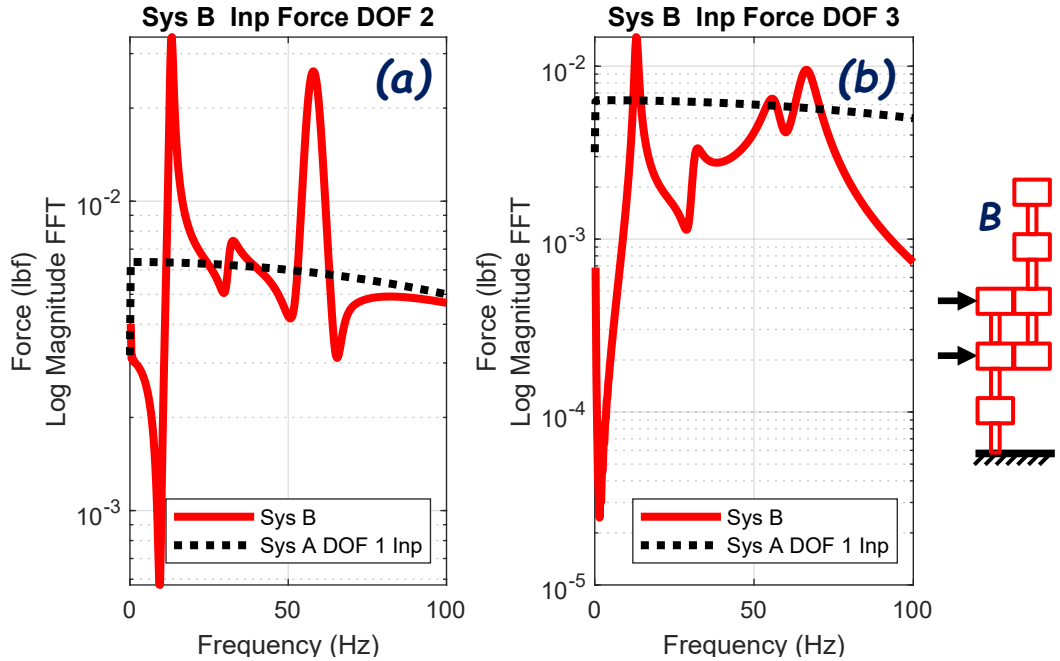

Figure 16. New system B force input spectra from the Modal FINE method to replicate DUT response from system A, plotted with the original system A input for reference. On the left (a) is shown the load derived for DOF 2 (m_2) and on the right (b) is the load for DOF 3 (m_3).

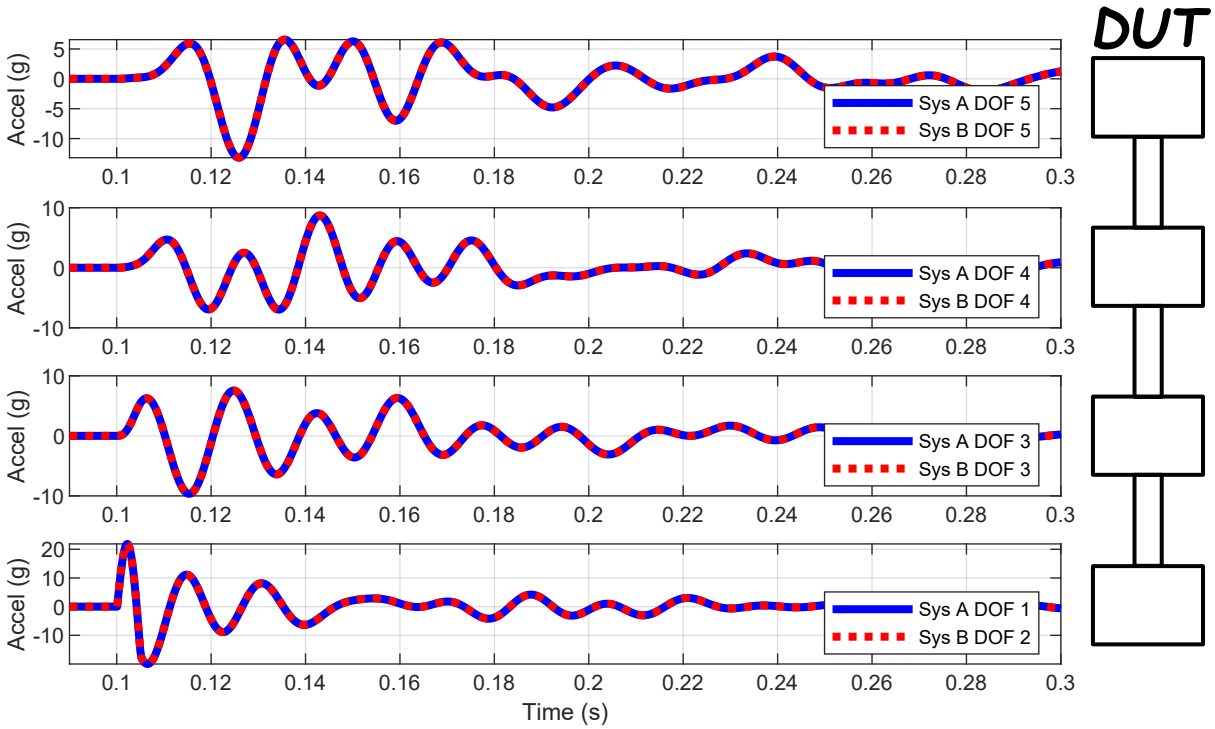

Figure 17. System B, DUT time history response with Modal FINE derived input compared to original DUT response in system A. The legend shows which system degree-of-freedom corresponds to each sub plot which in turn corresponds to the degrees-of-freedom in the DUT graphic to the right of the plots. The DUT responses are the same for both Systems.

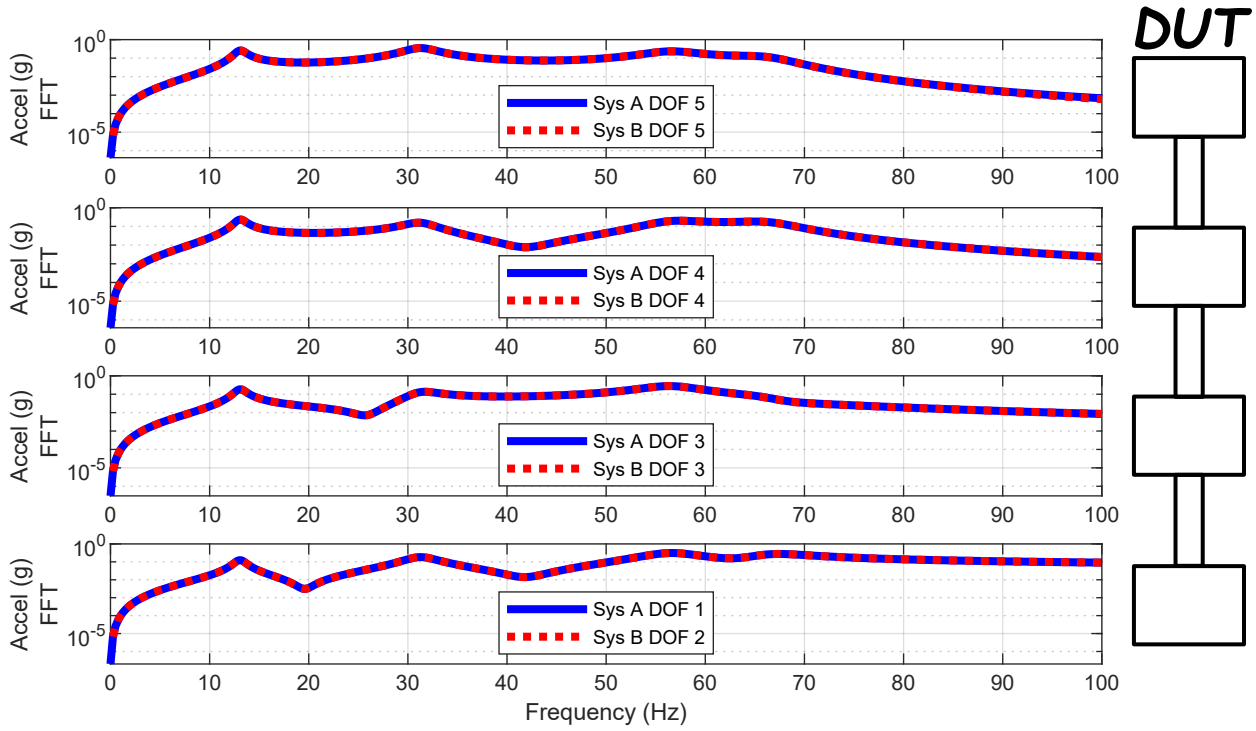

Figure 18. System B, DUT spectral response with Modal FINE derived input compared to original DUT response in system A. The legend shows which system degree-of-freedom corresponds to each sub plot which in turn corresponds to the degrees-of-freedom in the DUT graphic to the right of the plots. The DUT responses are the same for both Systems.

OBSERVATIONS AND FUTURE DIRECTION

The analytical model was used to show that using the same input for both field and laboratory configuration produces unmatching responses. If the goal is to match responses, then new loads must be derived. Using either of the FINE methodologies to account for the dynamic differences between configurations, the necessary loads to replicate field responses in laboratory configuration can be generated.

There must be at least as many DUT responses to match as active DUT connections. There must be at least as many test fixture inputs as active DUT connections. As an example, using 1 input load is insufficient to drive 2 connection degrees-of-freedom to reproduce DUT responses.

For the simple analytical model, both FINE methods produced laboratory DUT responses that match the field responses. In future work, these methods will be applied with data from tests. With test data there is an expectation that other factors like limited access to connection degrees-of-freedom, the ability to measure and excite rotary degrees-of-freedom, the ability to generate accurate FRFs, and the inconvenience of performing modal tests on each piece of hardware for every test setup will make using either of the FINE methods difficult. At that point, blending the methods, taking advantage of the strengths of each will result in an improved hybrid FINE method for reproducing field responses in the laboratory.

CONCLUSION

A history of vibration test specifications was provided. Over time the simple enveloped single axis specifications have advanced to MIMO testing. Newer MIMO FINE methods account for the dynamics of the DUT, the field, and the laboratory to generate new laboratory loads to replicate field responses. Theory was presented that is used in the FINE methods explored in the paper. A simple analytical model was used to substantiate initial claims that the FINE methods can be used to replicate field responses in the laboratory.

ACKNOWLEDGEMENTS

Some of the work presented herein was funded by Sandia National Laboratories.

Any opinions, findings, and conclusions or recommendations expressed in this material are those of the authors and do not necessarily reflect the views of the funding agency. The authors are grateful for the support obtained.

REFERENCES

[1] J. M. Reyes-Blanco, "Adjustment of Input Excitation to Account for Fixture – Test Article Dynamic Coupling Effects," University of Massachusetts Lowell, Lowell, Massachusetts, 2017.

[2] B. Zwink, "Dynamic Response Matching From Field To Laboratory Replication Methodology," University of Massachusetts Lowell, Lowell Massachusetts, 2020.

[3] United States Army Air Force, "Army Air Forces Specification No. 41065; Equipment: General Specification For Environmental Test Of," United States Army Air Forces, 1945.

[4] C. T. Morrow, "Some Special Considerations in Shock and Vibration Testing," in *The Shock and Vibration Bulletin*, Washington, D.C., 1956.

[5] R. E. Blake, "The Need to Control the Output Impedance of Vibration and Shock Machines," in *The Shock and Vibration Bulletin*, Washington, D.C., 1956.

[6] D. Rizzo and M. Blackburn, "The History of a Decision: A Standard Vibration Test Method for Qualification," *Journal of the IEST,* vol. 60, no. 1, p. 11, 2017.

[7] United States Air Force, "MIL-STD-810: Military Standard Environmental Test Methods for Aerospace and Ground Equipment," The United States Air Force, 1962.

[8] National Aeronautics and Space Administration (NASA), "Payload Vibroacoustic Test Criteria," Washington, DC 20546-0001, 2011.

[9] National Aeronautics and Space Administration (NASA), "Spacecraft Dynamic Environments Testing," Washington, DC 20546-0001, 2014.

[10] The Aerospace Corporation, "Test Requirements for Launch, Upper-Stage, and Space Vehicles," El Segundo, CA 90245-2808, 2006.

[11] Air Force Space Command, "Test Requirements for Launch, Upper-Stage and Space Vehicles," El Segundo, CA 90245, 2008.

[12] T. D. Scharton, "Force Limited Vibration Testing Monograph," NASA, JPL, Pasadena, CA, 1997.

[13] J. S. Cap, "Derivation of Parametric Limit Levels for Use in Developing a Response Limited Random Vibration Test," in *Spacecraft and Launch Vehicle Dynamic Environments Workshop*, El Segundo, 2007.

[14] T. J. Skousen, R. G. Coleman and D. O. Smallwood, "Response Limited Shaker Shock Testing," in *Proceedings of the 86th Shock and Vibration Symposium*, Orlando, FL, 2015.

[15] J. S. Cap, M. K. C de Baca and T. J. Skousen, "The Derivation of System Responses for a MIL-Standard Road," in *Proceedings of the 84rd Shock and Vibration Symposium*, Atlanta, GA, 2013.

[16] T. J. Skousen, J. S. Cap and M. K. C' de Baca, "The Derivation of System Shock Responses for a Worst-Case Road," in *Proceedings of the 85th Shock and Vibration Symposium*, Reston, VA, 2014.

[17] United States Department of Defense, "MIL-STD-810H: Department of Defense Test Methods Standard Environmental Engineering Considerations and Laboratory Tests," 2019.

[18] J. S. Cap, T. C. Togami and J. R. Hollingshead, "A Comparison of the Response of a Captive Carried Store to Both Reverberant Wave Acoustic Excitation and the Field Environment," in *Proceedings of the 67th Shock and Vibration Symposium*, Monterrey, CA, 1996.

[19] D. L. Gregory, J. S. Cap, T. C. Togami, M. A. Nusser and J. R. Hollingshead, "Multi-Exciter Vibroacoustic Simulation of Hypersonic Flight Vibration," in *Proceedings of the 70th Shock and Vibration Symposium*, Albuquerque, NM, 1999.

[20] J. S. Cap, D. G. Tipton and D. O. Smallwood, "The Derivation of Random Vibration Specifications from Field Test Data for Use With a Six Degree-of-Freedom Shaker Test," in *Proceedings of the 80th Shock and Vibration Symposium*, San Diego, CA, 2009.

[21] E. Habtour, G. S. Drake, A. Dasgupta, M. Al-Bassyiouni and C. Choi, "Improved Reliability Testing with Multiaxial Electrodynamics Vibration," in *Proceedings-Annual Reliability and Maintainability Symposium (RAMS)*, San Jose, CA, USA, 2010.

[22] P. M. Daborn, D. J. Ewins and P. R. Ind, "Replicating Aerodynamic Excitation in the Laboratory," in *IMAC 31*, Garden Grove, CA, 2013.

[23] P. M. Daborn, P. R. Ind and D. J. Ewins, "Enhanced ground-based vibration testing for aerodynamic environments," *Mechanical Systems and Signal Processing,* vol. 49, pp. 165-180, 2014.

[24] P. M. Daborn, C. Roberts, D. J. Ewins and P. R. Ind, "Next-Generation Random Vibration Tests," in *Topics in Modal Analysis II, Volume 8*, 2014, p. 397–410.

[25] P. M. Daborn, "Smarter Dynamic Testing of Critical Structures," University of Bristol, Bristol, England, 2014.

[26] R. L. Mayes, L. Ankers, P. Daborn, T. Moulder and P. Ind, "Optimization of Shaker Locations for Multiple Shaker Environments," *Experimental Techniques,* vol. 44, no. 3, pp. 283-297, 2020.

[27] R. Schultz, "Improving Efficiency of Multi-Shaker and Combined Shaker-Acoustic Vibration Tests," University of Massachusetts Lowel, Lowel Massachusetts, 2019.

[28] K. G. McConnell, "From Field Vibration Data to Laboratory Simulation," *Experimental Mechanics,* vol. 34, pp. 181-193, September 1994.

[29] P. Avitabile, "Why You Can't Ignore Those Vibration Fixture Resonances," *Sound and Vibration,* March 1999.

[30] J. M. Reyes-Blanco and P. Avitabile, "Force Customization to Neutralize Fixture-Test Article Dynamic Interaction," in *IMAC*, Orlando, FL, 2018.

[31] J. M. Reyes-Blanco, P. Avitabile, R. Jones and D. Soine, "Fixture Neutralization Method - Adjustment of Vibration Response to Account for Fixture-Test Article Dynamic Coupling Effects Using Measured Frequency Response Functions," in *IMAC XXXVII*, Orlando Florida, 2019.

[32] B. Zwink, P. Avitabile and D. G. Tipton, "Modal Projection Matching," in *IMAC XXXVII*, Orlando, Florida, 2019.

[33] P. Avitabile, Modal Testing: A Practitioner's Guide, 1st ed., Hoboken, NJ: Wiley, 2017.

[34] D. de Klerk, D. J. Rixen and S. N. Voormeeren, "General Framework for Dynamic Substructuring: History, Review and Classification of Techniques," *AIAA Journal,* vol. 46, no. 5, pp. 1169-1181, May 2008.

[35] R. L. Mayes, "A Modal Craig-Bamption Substructure for Experiments, Analysis, Control and Specifications," in *33rd International Modal Analysis Conference*, Orlando, FL, 2015.

[36] T. J. Skousen and R. L. Mayes, "Mechanical Environment Test Specifications Derived from Equivalent Energy in Fixed Base Modes," in *38th International Modal Analysis Conference*, Houston, TX, 2020.

[37] T. J. Skousen and R. L. Mayes, "Mechanical Environment Test Specifications Derived from Equivalent Energy in Fixed Base Modes, With Frequency Shifts from Unit-to-Unit Variability," in *39th International Modal Analysis Conference*, Virtual Conference, 2021.

[38] The MathWorks, Inc., *MATLAB - Matrix Analysis Software,* Natick, MA.